1.7 Å Structure of FR-1, a Fibroblast Growth Factor-Induced Member of the Aldo−Keto Reductase Family, Complexed with Coenzyme and Inhibitor[†,‡]

David K. Wilson,[§] Takayuki Nakano,[∥] J. Mark Petrash,[∥] and Florante A. Quiocho*[,§]

Howard Hughes Medical Institute and Department of Biochemistry, Baylor College of Medicine, One Baylor Plaza, Houston, Texas 77030, and Department of Ophthalmology and Visual Sciences, Washington University School of Medicine, 660 South Euclid Avenue, St. Louis, Missouri 63110

Received August 1, 1995; Revised Manuscript Received September 5, 1995[⊗]

ABSTRACT: Murine FR-1 is a protein that is induced by fibroblast growth factor-1 and, therefore, may play a role in the regulation of the cell cycle. Sequence comparison indicates that it is a member of the NADPH-dependent aldo−keto reductase family. It bears 70% identity to human aldose reductase, an enzyme implicated in diabetic complications and a target for drug design. We have determined the 1.7 Å resolution structure of the FR-1 in a ternary complex with NADPH and zopolrestat, a potent aldose reductase inhibitor. FR-1 folds into a $(\beta/\alpha)_8$ barrel with an active site characterized by a preponderance of hydrophobic residues residing in a deep oblong cavity at the C-terminal end of the β-barrel. The nicotinamide moiety of the coenzyme sits in the base of the cavity. Zopolrestat occupies the active site cavity and makes numerous contacts with several hydrophobic residues. The FR-1 ternary complex structure indicates that it uses the same general catalytic mechanism as aldose reductase and other members of the family whose structures have been determined. The protein exhibits reductase activity with DL-glyceraldehyde as a substrate and is strongly inhibited by zopolrestat. When compared with the structure of a similar ternary complex of aldose reductase, the binding site retains many of the interactions with the coenzyme and inhibitor from the conserved residues. Some differences in sequence, however, create a larger binding site that contains six more water molecules than in the aldose reductase ternary complex structure. Sequence comparisons with other members of this family of proteins in a structural context show high conservation of active site architecture.

The aldo−keto reductase family comprises a group of proteins having similar primary structures and physical properties. Expressed as M_r ~36 000 monomers, these proteins have been purified from a wide variety of vertebrate tissues, plants, and prokaryotic organisms. Most but not all members of this protein family catalyze the NADPH-dependent reduction of a diverse and overlapping range of carbonyl substrates (e.g., monosaccharides, steroids, prostaglandin, aliphatic aldehydes, and xenobiotic compounds). As a group, these aldo−keto reductases may play a beneficial role in detoxification of naturally occurring carbonyls such as 3-deoxyglucosone (Kanazu *et al.*, 1991) and glyoxal (Vander Jagt *et al.*, 1992).

Aldose reductase (ALR2)[1] is one of the best studied of the aldo−keto reductases. Interest in this enzyme stems from the observation that its role in converting glucose to sorbitol may be important in the pathogenesis of some diabetic complications such as retinopathy, neuropathy, and nephropathy (Kinoshita & Nishimura, 1988). Interruption of this accessory pathway of glucose metabolism through inhibition of ALR2 provides an attractive therapeutic strategy for prevention of some diabetic complications.

High-resolution crystallographic analyses of human ALR2 holoenzyme and its ternary complex with zopolrestat have provided atomic-level details of the architecture of the enzyme family and the precise geometry of coenzyme and inhibitor binding (Wilson *et al.*, 1992, 1993; Borhani *et al.*, 1992). Moreover, these structures have provided insights into the catalytic mechanism and paved the way for probing catalytic function by site-directed mutagenesis. ALR2 adopts a $(\beta/\alpha)_8$ barrel structural motif with a large hydrophobic active site consistent with observations that many of its best substrates are hydrophobic compounds such as aromatic aldehydes and steroids (Wermuth & Monder, 1983). Zopolrestat, one of many clinically relevant potent aldose reductase inhibitors that possess marked hydrophobic character (Mylari *et al.*, 1991; Sarges, 1989; Sarges & Oates, 1993), binds in the active site, making extensive contacts with hydrophobic residues.

Recent demonstration that 3α-hydroxysteroid dehydrogenase (3α-HSD) (Hoog *et al.*, 1994) and aldehyde reductase (ALR1) (El-Kabbani *et al.*, 1994) also fold with the same $(\beta/\alpha)_8$ barrel motif indicates that members of the aldo−keto reductase family will most likely share this structure. Mutagenesis and kinetic studies on ALR2 and ALR1 (Tarle *et al.*, 1993; Bohren *et al.*, 1994; Kubiseski *et al.*, 1994; Morjana *et al.*, 1989) and 3α-HSD (Pawlowski & Penning,

[†] Supported in part by NIH Grants EY05856, P30EY02687, and P60DK20579 and by an unrestricted grant to the Department of Ophthalmology and Visual Sciences from Research to Prevent Blindness, Inc.

[‡] Coordinates have been deposited in the Protein Data Bank (file name 1FRB).

* Investigator of the Howard Hughes Medical Institute and to whom correspondence may be addressed.

[§] Howard Hughes Medical Institute and the Department of Biochemistry, Baylor College of Medicine.

[∥] Department of Ophthalmology and Visual Sciences, Washington University School of Medicine

[1] Abbreviations: FR-1, fibroblast growth factor-1 regulated protein; ALR2, aldose reductase; ALR1, aldehyde reductase; 3α-HSD, 3α-hydroxysteroid dehydrogenase.

0006-2960/95/0434-14323$09.00/0

1994) provide additional evidence for conservation of many of the catalytic residues at the active site.

While similarities in catalytic and functional properties initially formed the basis for grouping the aldo−keto reductases into a distinctive class of proteins (Bachur, 1976), additional proteins with a significant degree of sequence identity with the aldo−keto reductases have recently been identified through DNA cloning studies. A major protein expressed in the adult mouse vas deferens, designated MVDP (mouse vas deferens protein), is characterized by ~69% identity to murine aldose reductase (Pailhoux *et al.*, 1990; Gui *et al.*, 1995). Murine NIH 3T3 cells express a similar protein, designated FR-1, which shares ~69% identity with murine aldose reductase and ~82% identity with MVDP (Donohue *et al.*, 1994). FR-1 and MVDP are unique among the aldo−keto reductases in that their expression appears to be transcriptionally regulated by polypeptide growth factors and androgens, respectively (Pailhoux *et al.*, 1990; Donohue *et al.*, 1994). Despite their sequence similarity to aldose reductase, aldo−keto reductase activity has not been reported for either FR-1 or MVDP. Since most proteins within this family function as oxidoreductases, we sought to determine the crystal structure of FR-1 and to examine whether it has enzymatic activity and if this activity can be modulated by inhibitors which are known to bind to ALR2.

MATERIALS AND METHODS

FR-1 Expression and Purification. Murine FR-1 was obtained by overexpression of the cDNA in *Escherichia coli*. For construction of the expression plasmid pMON/FR-1, an *Nco*I-*Hin*dIII restriction fragment containing the entire coding sequence for FR-1 (Donohue *et al.*, 1994) was ligated into pMON20,400, an expression plasmid used previously to overexpress human aldose reductase (Tarle *et al.*, 1993). Recombinant FR-1 was extracted from host cells by treatment with DNase and lysozyme as described previously (Merck *et al.*, 1992) and was subsequently purified to homogeneity by a method described for human aldose reductase (Petrash *et al.*, 1993) with the exception that chromatography over DEAE-Sephadex was used in the place of chromatofocusing.

Enzyme Assay and Inhibitor Binding. Aldo−keto reductase activity in purified fractions was determined spectrophotometrically as for aldose reductase (Tarle *et al.*, 1993) using 5 mM DL-glyceraldehyde and 0.15 mM NADPH as substrate and coenzyme, respectively. The apparent K_m value was determined at 25 °C in 50 mM potassium phosphate, 10 mM KCl, and 0.5 mM EDTA at pH 7.0. Initial steady-state velocity data were fitted to the Michaelis−Menten equation.

The inhibition constant was determined using 10 mM DL-glyceraldehyde and 0.15 mM NADPH. The initial steady-state velocity *vs* concentration of zopolrestat was analyzed by nonlinear least-squares analysis as described by Cha (1975).

The dissociation constants for various FR-1−ligand complexes were determined spectrofluorometrically at 25 °C by measuring quenching of intrinsic protein fluorescence or energy transfer fluorescence to the dihydronicotinamide moiety of NADPH. Excitation and emission wavelengths of 280 and 330 nm, respectively, were used for the determination of the dissociation constants for NADPH and $NADP^+$ and the apoenzyme. For the measurement of dissociation constants for zopolrestat with the enzyme−NADPH complex and for NADPH with the enzyme−zopolrestat complex, the excitation and emission wavelengths were set to 282 and 450 nm, respectively. The concentration of FR-1 used for these determinations was approximately 0.1−1 μM.

Crystallization and Structure Determination. The procedure used for the crystallization of the FR-1 in the presence of NADPH and zopolrestat was essentially identical to that used for the human aldose reductase ternary complex (Wilson *et al.*, 1993). The space group was determined to be $P2_12_12_1$, and the unit cell dimensions were $a = 59.45$ Å, $b = 65.38$ Å, and $c = 90.29$ Å with one molecule per asymmetric unit. Diffraction intensities to 1.7 Å resolution were collected from a flash-frozen crystal (−130 °C liquid nitrogen stream) on an SDMS dual multiwire detector system mounted on a Rigaku RU200 X-ray generator (fine focused Cu Kα) equipped with a graphite crystal monochromator and operated at 110 mA and 40 kV. A total of 213 331 reflections was measured which, after merging, resulted in 43 337 unique reflections and an overall R_{merge} of 4.61% calculated on intensity. Final refinement used 36 797 reflections between 8.0 and 1.7 Å resolution with $F > \sigma(F)$. This comprised 94.3% of the reflections within that resolution range and 90.0% of the possible reflections between 1.8 and 1.7 Å.

Phase determination was accomplished via molecular replacement as implemented by the X-PLOR package of programs (Brünger, 1992). The search model was the 1.4 Å resolution structure of the human aldose reductase−NADPH (holoenzyme) complex (D. K. Wilson, J. M. Petrash, and F. A. Quiocho, unpublished data). The rotation function was calculated using intensities between 20.0 and 6.0 Å and Patterson vectors ranging from 5.0 to 30 Å. A Patterson correlation refinement affirmed that the highest peak in the rotation function (located at Euler angles of $\theta_1 = 234°$, $\theta_2 = 72°$, $\theta_3 = 147°$) was the rotation solution. The highest translation peak appeared at 17.78, 28.09, and 11.73 Å and was applied to the rotated molecule. Rigid body refinement using 7042 reflections between 10.0 and 3.0 Å reduced the crystallographic *R*-factor from 0.502 to 0.457. Iterations of positional and temperature factor refinement using the X-PLOR package followed by manual refitting of protein atoms, using the CHAIN program (Sack, 1988), and inclusion of zopolrestat atoms and 448 ordered water molecules yielded the final structure.

RESULTS AND DISCUSSION

FR-1 Structure. FR-1 consists of 315 amino acids (less the initiator methionine that is not seen in the well-ordered N-terminus of the protein) and an approximate molecular mass of 36 000 Da. The structural refinement to 1.7 Å resolution converged at a crystallographic *R*-factor of 0.158 for the model consisting of 3062 non-hydrogen atoms (2537 protein, 48 NADPH, 29 zopolrestat, and 448 water molecules). The root-mean-square deviations from ideal bond lengths and bond angles were calculated to be 0.008 Å and 1.78°, respectively. The density for almost all the protein non-hydrogen atoms and all of the coenzyme and inhibitor atoms is exceptionally well-defined. This is exemplified by the difference electron density map of the bound zopolrestat drug (Figure 1). Not one residue is within the disallowed regions in a Ramachandran plot.

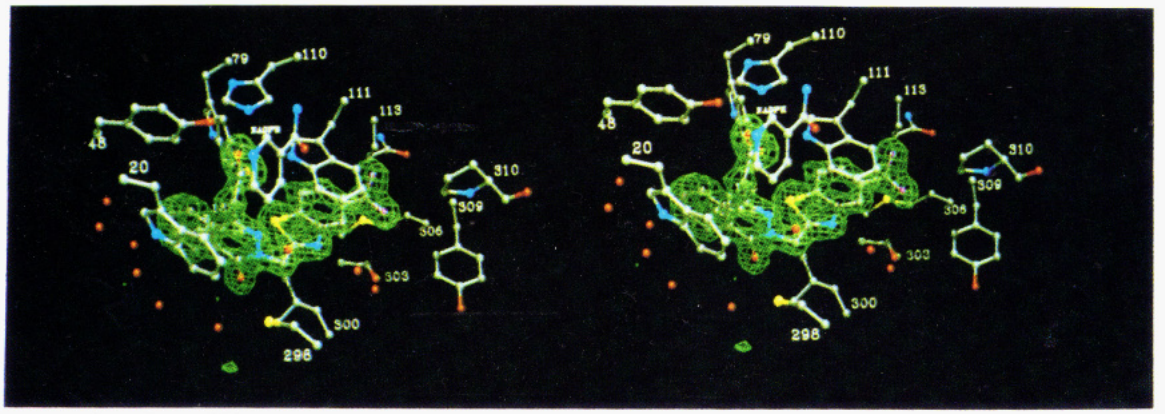

FIGURE 1: Stereoview of the difference electron density (green) of the zopolrestat contoured at 3σ and superimposed refined structure in the region of the active site. Difference density was calculated using the coefficients ($|F_o - F_c|$) and α_c phases derived from the 1.7 Å resolution refined structure but omitting the inhibitor atoms. This figure and Figures 2B, 5, and 6 were prepared using the program MIDASplus (Ferrin *et al.*, 1988).

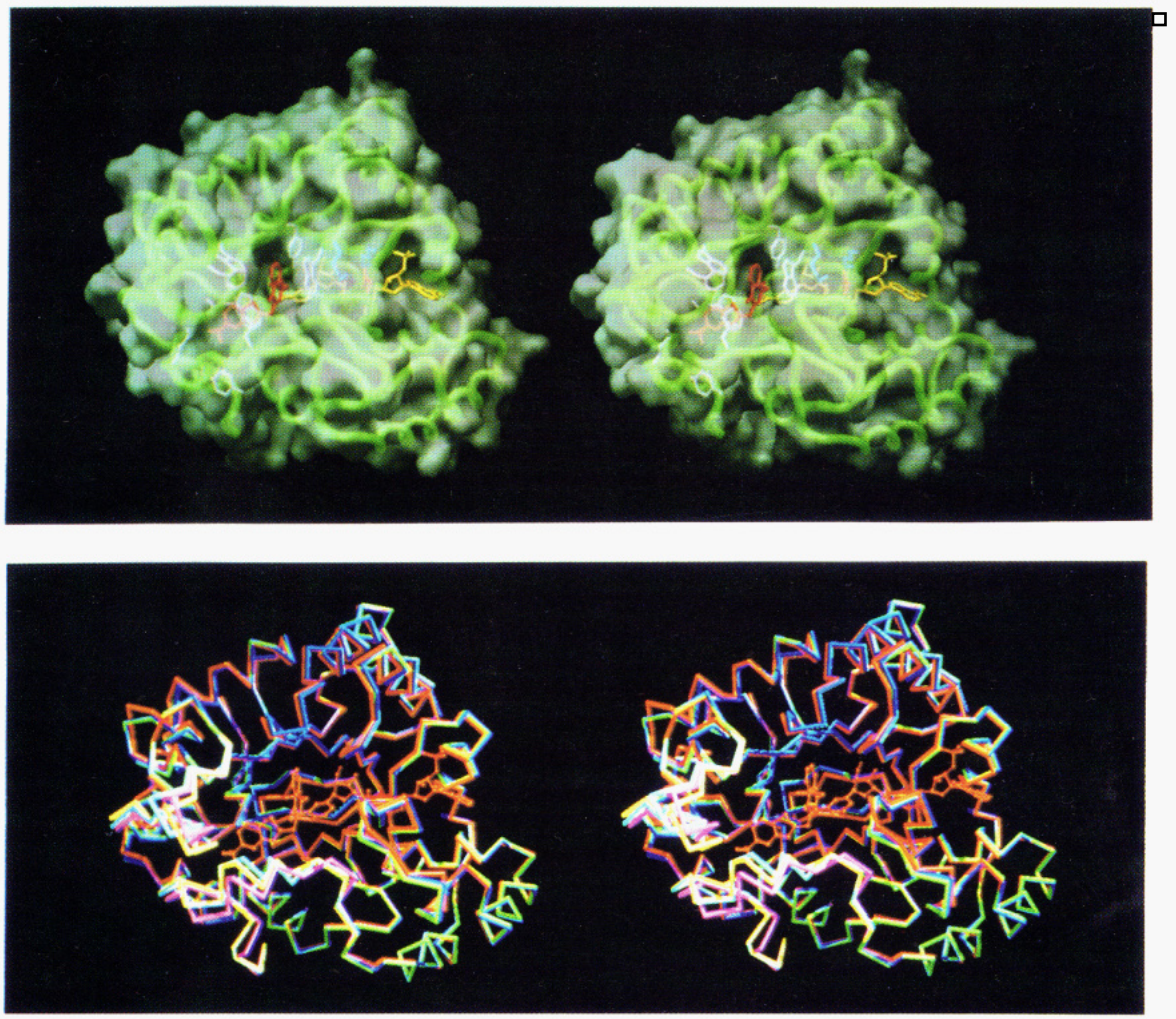

FIGURE 2: Stereoview of the structure of the ternary FR-1−NADPH−zopolrestat complex. (A, top) Translucent molecular surface (gray) of the complex as calculated and presented by GRASP (Nicholls *et al.*, 1991). The buried Cα backbone trace is shown in green. The NADPH (especially the adenosine in a pocket and the amide of the nicotinamide in the central active site pocket) is shown in yellow and zopolrestat (especially the phthalazinone ring in the active site pocket) is in red. The buried hydrophobic active site residues are colored white, and charged residues forming the "belt" over the NADPH pyrophosphate are colored blue for basic and red for acidic residues. (B, bottom) Superimposed Cα backbone traces of the FR-1 ternary complex (red/magenta), the ALR2−NADPH binary complex or holoenzyme (blue/cyan), and the ALR2−NADPH−zopolrestat ternary complex (green/yellow). Only the zopolrestat and NADPH bound to FR-1 are shown; the inhibitor is to the left of the fully extended NADPH. The large conformational difference involving the segments containing residues 121−135 and 295−315 between the structures can be seen in the lower left-hand corner and is highlighted by magenta, cyan, and yellow traces.

FR-1 folds into a $(\beta/\alpha)_8$-barrel motif (Figure 2), similar to previously determined structures of three other members of the aldo−keto reductase family—human ALR2 (Wilson *et al.*, 1992; Borhani *et al.*, 1993), 3α-HSD (Hoog *et al.*, 1994), and ALR1 (El-Kabbani *et al.*, 1994). The conservation of this structure, as well as considerable sequence

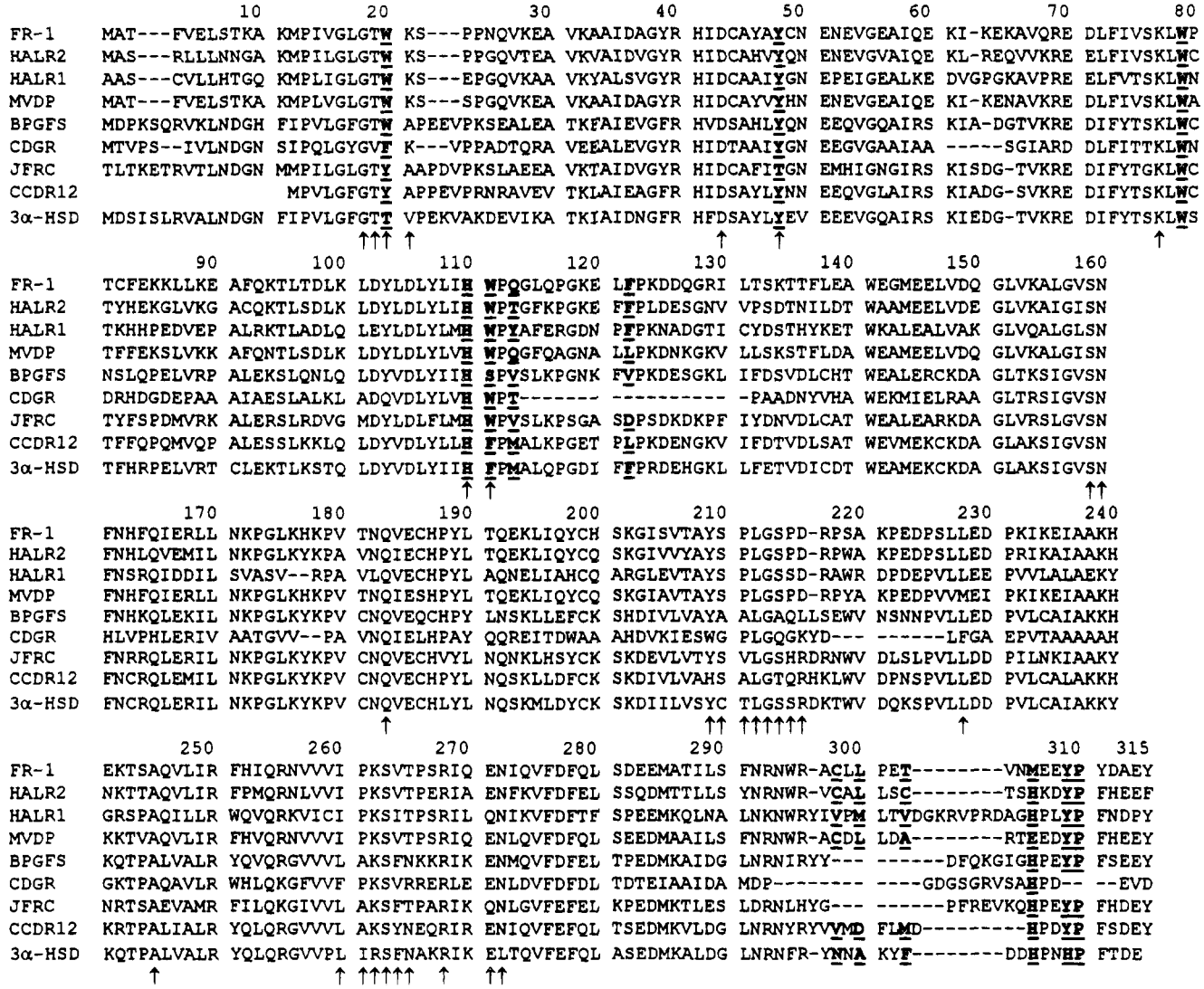

FIGURE 3: Alignment of the sequences of the aldo−keto reductase family highlighting the residues making ≤4 Å contacts with NADPH (arrows) and zopolrestat (underlined and bold) based on the FR-1 ternary complex structure. Abbreviations used are as follows: FR-1, human FR-1 (Donohue *et al.*, 1994); HALR2, human aldose reductase (Bohren *et al.*, 1989); HALR1, human aldehyde reductase (Bohren *et al.*, 1989); MVDP, murine vas deferens protein (Pailhoux *et al.*, 1990); BPGFS, bovine prostaglandin F synthase (Watanabe *et al.*, 1988); CDGR, *Corynebacterium* diketogluconate reductase (Anderson *et al.*, 1985); JFRC, Japanese frog ρ crystallin (Fujii *et al.*, 1990); CCDR12, human chlordecone reductase (Winters *et al.*, 1990); 3αHSD, 3α-hydroxysteroid dehydrogenase (Pawlowski *et al.*, 1991).

identity among members (Figure 3), establishes the structural motif of this protein family. This motif has been found in the structures of at least 30 enzymes that exhibit greatly differing activities and sequences lacking in significant homology (Brändén, 1991). As with the ALR2, 3α-HSD, and ALR1, the N-terminal end of the β-barrel of FR-1 is capped by a β-hairpin, and two extra helices are inserted after strand 7 and helix 8 to break the regularity of the barrel's secondary structure.

Root-mean-square deviations calculated pairwise between the α-carbons of the ternary FR-1−NADPH−zopolrestat complex and the similar ternary complex of ALR2 (Wilson *et al.*, 1993) and the 1.4 Å structure of the ALR2−NADPH binary complex were 0.82 and 0.83 Å, respectively (Figure 2B). This close similarity of structures is not surprising since FR-1 and ALR2 share approximately 70% sequence identity (Figure 3).

By virtue of the proximal locations of the nicotinamide ring of the bound NADPH and the bound zopolrestat drug (discussed below), the active site of FR-1 is confined to a deep oblong cavity at the C-terminal end of the β-barrel (Figure 2), consistent with the ALR2 and ALR1 structures as well as with other known enzymes with the $(\beta/\alpha)_8$-barrel motif.

NADPH Binding. FR-1 shares functional similarity with the other members of the aldo−keto reductase family. Indeed, well-defined density corresponding to the coenzyme was observed in a site completely analogous to the NADPH binding site in ALR2 holoenzyme structure (Wilson *et al.*, 1992). The coenzyme, with 91% of its solvent-accessible surface buried, is bound in an extended conformation with the nicotinamide moiety forming part of the base of the active site cavity (Figure 2). The pyrophosphate straddles the lip of the barrel, and the adenosine fits in a shallow cavity at the edge of the barrel. The pyrophosphate is sequestered by a belt consisting of residues 214−228. This "locks" over the coenzyme using Asp 216 on the loop to engage in salt links with Lys 21 which is located at the C-terminal end of β1 and Lys 262 on β8 (Figure 2A).

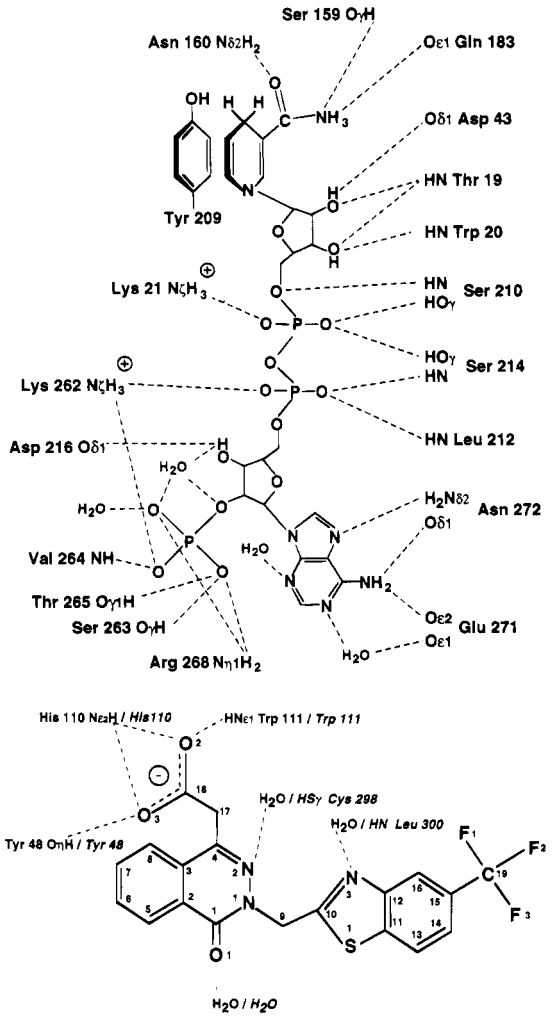

FIGURE 4: Schematic diagrams depicting (dashed lines) the hydrogen bonds (≤3.3 Å distance) and salt links between FR-1 and NADPH (A, top) and zopolrestat (B, bottom). Not shown in (A) and (B) are 27 and 5 polar interactions, respectively, that significantly exceed the hydrogen bond cutoff distance and are therefore included in the van der Waals contacts. In the complex with zopolrestat (B), residues and waters from FR-1 are listed first, followed by those (italics) from ALR2. Note that in the ARL2 ternary complex Thr 113 γ1OH donates a bifurcated hydrogen bond to two of the fluorine atoms (Wilson *et al.*, 1993).

A large number of contacts (250) of ≤4 Å are formed between atoms of NADPH and FR-1. Of these contacts 30 are hydrogen bonds (distances ≤3.3 Å), including 4 which are also involved in salt links (Figure 4A). The remaining 220 contacts are attributed to van der Waals interactions.

On the basis of our structural data, two important functional features are conserved between FR-1 and ALR2. A 4-*pro-R* hydride transfer stereospecificity is one feature predicted on the basis of two critical interactions revealed in the structure. The hydrogen-bonding interactions between the amide group of the nicotinamide moiety and side chains from Ser 159, Asn 160, and Gln 183 direct the B-face of the nicotinamide to the active site cavity (Figure 4A). The stacking interaction between the A-face of the nicotinamide ring and Tyr 209, resulting in 35 van der Waals contacts, also fixes the nicotinamide orientation (Figure 5). The interactions that confer preference for NADPH over NADH are also conserved. The most dominant of these are the salt links to the 2′-phosphate made by Lys 262 and Arg 268, which are also involved in fastening the flap over the pyrophosphate as described above.

Catalysis. The functional similarity of FR-1 with ALR2, ALR1, and 3α-HSD extends to the catalytic activity of these enzymes. The forward reaction catalyzed by the aldo−keto oxidoreductase family consists of a hydride transfer from the nicotinamide moiety of the NADPH to a carbonyl carbon of the substrate concomitant with the abstraction of a proton by the carbonyl oxygen from a general acid. The initial high-resolution structural studies of ALR2 have revealed up to three possible candidates for the general acid: Tyr 48, His 110, and Cys 298 in ALR2 (Wilson *et al.*, 1992, 1993). Subsequent structure determination of 3α-HSD also identified residues analogous to the Tyr and His residues (Tyr 55 and His 117, respectively) (Hoog *et al.*, 1994). The three residues in ALR2 are completely conserved in FR-1 (Figures 3 and 5). In all three enzymes, the tyrosine is favored as a proton donor since it is engaged in a hydrogen-bonding interaction with Lys 77 that is in turn salt linked and hydrogen bonded with Asp 43 in ALR2 and FR-1 (Figure 5). A similar arrangement is seen with the corresponding residues in 3α-HSD (Hoog *et al.*, 1994). As originally proposed (Wilson *et al.*, 1992, 1993), the primary function of this charge relay system is to depress the pK_a of the tyrosine, thereby facilitating proton transfer from the phenolic hydroxyl group and stabilizing the incipient phenoxide specie. It is unlikely that the histidine is able to perform this function since its pK_a is expected to be depressed by the hydrophobic nature of its surroundings, which include the aliphatic portion of the Lys 77 side chain as well as side chains from Ala 45, Tyr 48, Trp 79, and Trp 111. Since Cys 298 is not present in other catalytically active aldo−keto reductases (e.g., 3α-HSD) (Figure 3), it can be ruled out as a possible general acid. Although the distance from Cys Sγ to the C4 of the NADPH is only 3.87 Å in the case of the ALR2 holoenzyme and 3.91 Å in the ALR2 ternary complex, this distance is dramatically longer (7.44 Å) in the FR-1 ternary structure. Analysis of site-directed mutants of ALR2 (Tarle *et al.*, 1993; Bohren *et al.*, 1994) and 3α-HSD (Pawlowski & Penning, 1994) confirms the role of the tyrosine as the general acid as well as the importance of the residues involved in the charge relay system. Mutants at His 110 indicated that it plays a significant role in catalysis, possibly in the orientation of substrates (Tarle *et al.*, 1993; Bohren *et al.*, 1994).

Although the enzymology of FR-1 has not yet been studied in detail, it clearly has NADPH-dependent reductase activity when assayed with DL-glyceraldehyde (K_m of 0.92 ± 0.1 mM). At pH 7.0, tight binding of NADPH and $NADP^+$ to FR-1 was also observed, with K_d values of 0.45 ± 0.03 and 0.23 ± 0.02 μM, respectively. The similarity of the belt which folds over the pyrophosphate of the NADPH with the belt in ALR2 suggests that FR-1 will also follow an ordered bi-bi mechanism. The NADPH coenzyme would bind first, followed by the conformational change associated with the loop. The substrate would then bind and undergo reduction, and the product would dissociate. Binding of substrate may also be accompanied by conformational change (see below; Wilson *et al.*, 1993). Finally, the $NADP^+$ would dissociate with the accompanying loop movement in preparation for another catalytic cycle. This last step has been shown to be the rate-limiting step in the reaction (Grimshaw *et al.*, 1990).

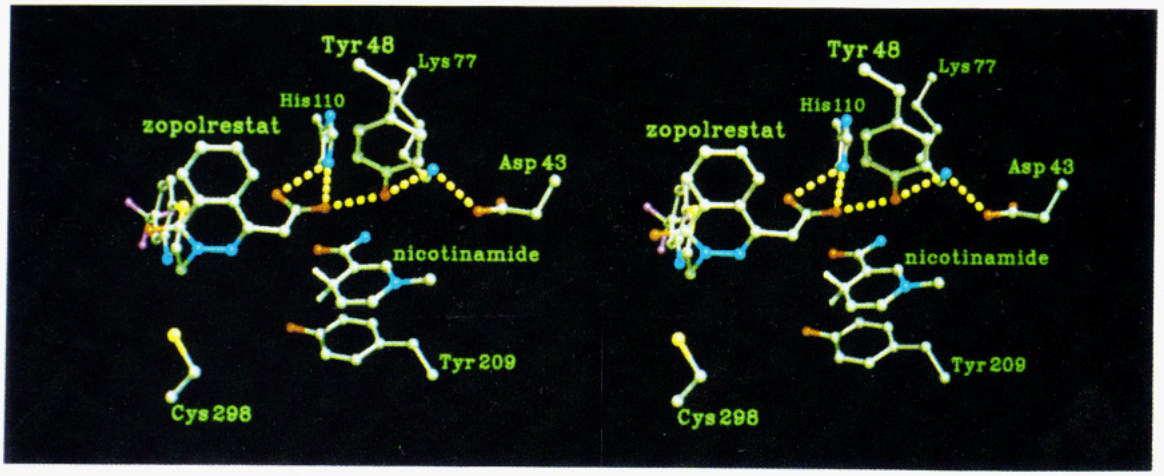

FIGURE 5: Stereoview of the residues involved in the catalytic function of FR-1, which are identical to those of ALR2 (Wilson *et al.*, 1993). Discussed in the text is the importance of the triad of interactions consisting of a hydrogen bond of Tyr 48, the proposed proton donor in the forward reaction, with Lys 77 which in turn makes a hydrogen bond and salt link with Asp 43.

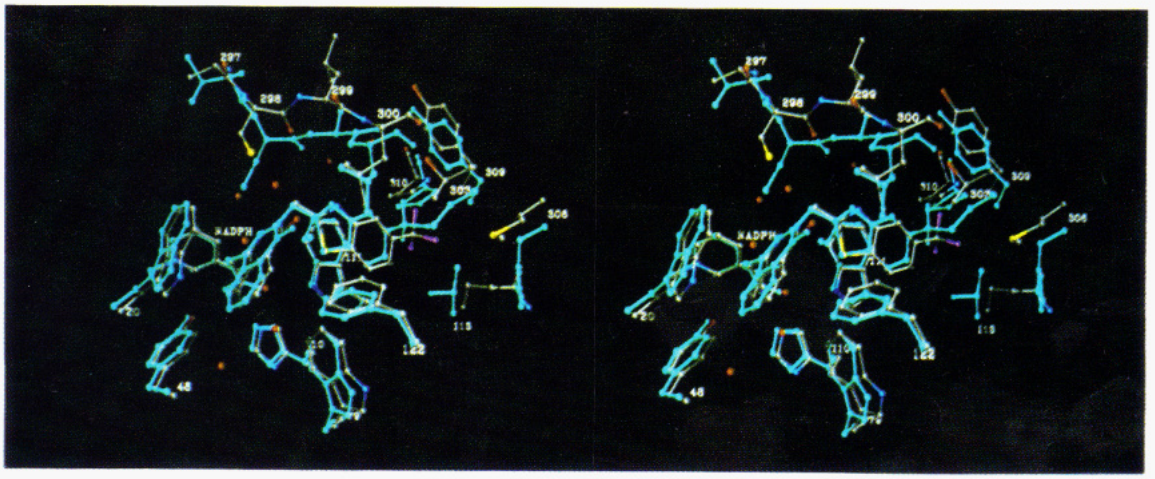

FIGURE 6: Stereoview of the superimposed active sites (centered at the bound zopolrestat) of the ternary complexes of FR-1 (color by atom types) and of ALR2 (cyan). Only the nicotinamide ring of NADPH is shown to the left of the phthalazinone ring of the inhibitor. Shown is the conformational difference of the segment from residues 297 to 300. This difference extends to the carboxy-terminal end (Figure 2B) deploying residues including (this figure) Thr 303, Met 306, and Tyr 309 of FR-1 that are equivalent to Cys, His, and Tyr, respectively, in ALR2.

Inhibitor Binding. Zopolrestat is one of a large number of inhibitors developed as potential drugs to combat complications arising from diabetes by inhibiting ALR2 (Mylari *et al.*, 1991; Sarges & Oates, 1993). While the exact role of aldose reductase in the pathogenesis of diabetic complications is not clear, there is abundant experimental evidence supporting the therapeutic rationale for clinical use of aldose reductase inhibitors (Sarges & Oates, 1993). Although little is currently known about the enzymatic properties or biological role of FR-1, its active site is clearly occupied by the drug (Figures 1 and 2) in a manner very similar to that seen in the ternary ALR2−NADPH−zopolrestat complex (Figure 6) (Wilson *et al.*, 1993). Moreover, like human aldose reductase, FR-1 was strongly inhibited by zopolrestat (K_i of 17 ± 10 nM). Zopolrestat bound tightly to the FR-1 with a dissociation constant (K_d) of 30 ± 10 nM in the presence of NADPH. The crystallographic data do not support inhibition and competition studies implicating that zopolrestat, as well as many other inhibitors, binds to a site independent of the substrate- and NADPH-binding sites (Sarges, 1989; Kador & Sharpless, 1983).

Zopolrestat and NADPH, together, almost extend the full diameter of the barrel (Figure 2). The phthalazinone ring is positioned close to the nicotinamide ring in the large active site cavity. The benzothiazole ring is directed away from the center and sequestered in a small pocket formed by segments of strands 4 and 5 of the β-barrel and a meander composed of residues 295−303 near the C-terminal end of the protein. The relative orientation of these ring systems is slightly modified from that in the ALR2-bound structure. The N2−N1−C9−C10 and N1−C9−C10−S1 (Figure 4B) torsion angles are −89° and −9°, respectively, for the FR-1 complex *versus* −85° and −16°, respectively, for those in the ALR2 complex. Comparing these values with those of the small molecule crystal structure of the drug (−81° and −51°, respectively) (Mylari *et al.*, 1991) indicates torsion changes upon binding for maximal steric fit of the drug in the active site.

The inhibitor, with 92.8% of its accessible surface buried, makes a total of 127 contacts of less than 4 Å, 105 with 13 residues and 22 with 9 bound water molecules. Only seven hydrogen bonds (≤3.3 Å), one also being a salt link, contribute to the total number of contacts (Figures 4B and 6); the rest are made up by van der Waals interactions. Only the water hydrogen bonded to N3 (Figure 4B) is in turn hydrogen bonded to FR-1 (Cys 299 O and Tyr 311 Oη).

As first observed in the ALR2 structure (Wilson *et al.*, 1993), the bulk of the interactions between the drug and FR-1

involves hydrophobic residues. This is in agreement with the presence of an unusually large number of hydrophobic residues in the active sites of both proteins. Many of these residues (Trp 20, Tyr 48, Trp 79, Trp 111, Phe 122, Leu 300, Met 306, Tyr 309, and Pro 310) make a total of 92 van der Waals contacts (mostly hydrophobics) with the zopolrestat (Figures 1, 2A, and 6). Many of the dominant interactions are shown in Figures 1 and 6. The benzothiazole ring is sandwiched between Trp 111 which makes 40 contacts and Leu 300 which makes 10 contacts. The phthalazinone ring is seen observed stacking against Trp 20, making a total of 19 contacts. The interactions of the carboxylate of the inhibitor with His 110 and Tyr 48 are also preserved (Figures 4B, 5, and 6).

Despite the hydrophobic nature of the active site, six ordered water molecules which are not present in the ALR2 structure are seen (Figures 1 and 6). These waters are, for the most part, buried and reflect the fact that the FR-1 active site is somewhat larger than that of ALR2. Superimposing the active site of ALR2 on FR-1 shows that the conformational differences between the two enzymes are largely confined to the segment of residues between 295 and 315 (Figures 2B and 6). This region, which has previously been shown to be flexible (Wilson *et al.*, 1993), is also characterized by pronounced sequence divergence (Figure 3). This overlap shows that this loop is positioned even farther away from the zopolrestat molecule, creating a space in the active site of FR-1 which is occupied by four water molecules (Figures 2B and 6). Another loop, composed of residues 121−135, has been shown to flex upon inhibitor binding to ALR2 holoenzyme (Wilson *et al.*, 1993). This loop also adopts a slightly different conformation in FR-1. The flexibility of these loops is likely to play a role in determining the substrate specificity of these enzymes and modulating inhibitor binding.

The differences in the interactions with zopolrestat observed in the FR-1 and ALR2 ternary complex structures are mainly due to the aforementioned structural difference in the loop near the C-terminal end (residues 295−315), thereby creating the following consequences (Figures 2B, 4, and 6). The thiol group of Cys 298 and the amide side-chain nitrogen of Leu 300, which donate hydrogen bonds to N2 and N3, respectively, of zopolrestat bound in ALR2, have both been replaced by water molecules in FR-1. The loop conformation adopted by FR-1 causes the side chain of Cys 298 to extend into the volume occupied by Trp 219 in ALR2. Trp 219 is replaced by a much less bulky Ser in FR-1. The α-carbons for Cys 298 and Leu 300 are displaced by 1.3 and 2.8 Å, respectively, between the two structures. The hydrogen-bonding scheme around the trifluoromethyl group has also changed as a result of sequence differences. Rather than accepting a bifurcated hydrogen bond from Thr 113 in ARL2, which is a Gln residue in FR-1, the phthalazinone ring of the inhibitor bound in FR-1 is shifted slightly relative to its position in ALR2 so that none of the fluorine atoms can accept a hydrogen bond from the protein (Figures 4 and 6).

Sequence Comparison with Other Members of the Aldo−Keto Reductase Family. Examination of the FR-1 sequence aligned with eight different members of the aldo−keto reductase family sheds light on the ability of each protein to bind NADPH and zopolrestat, as well as to express catalytic activity (Figure 3). Furthermore, this alignment indicates that many of the conserved residues (Trp 20, Tyr 48, Trp 79, His 110, Trp 111, Leu 300) are among the ones involved in key interactions with zopolrestat binding.

The structures of the ternary complexes of FR-1 and ALR2 can be used to identify the key residues involved in NADPH binding. Residues critical in binding and orienting the nicotinamide ring, Ser 159, Asn 160, and Tyr 209, are almost completely identical. Only Tyr 209 is conservatively substituted by Trp and His residues in diketogluconate reductase (CDGR) and chlordecone reductase (CCDR12), respectively. Lys 262 is salt linked to the 5′-phosphate of adenosine and is primarily responsible for recognizing and binding the 2′-phosphate along with Arg 268. Both of these residues are conserved within the family (3α-HSD has Arg substituted for Lys 262). The belt which folds over the pyrophosphate is fastened by salt links involving Asp 216 on the loop and Lys 21 and Lys 262. While Lys 262 is very much conserved, as described above, Lys 21 and Asp 216 are conspicuously absent in approximately half of the family. This suggests the possibility of such a belt being absent or somewhat altered in these enzymes. One such enzyme is 3α-HSD, which is known to bind NADPH.

In the absence of the structure of a complex with a substrate analog, we have used the residues making contacts with zopolrestat in the FR-1 and ALR2 structures to define the residues which are potentially involved in substrate binding. The sequence alignment shows that 9 of 13 of them maintain at least 50% identity across the family. However, as indicated above, the residues associated with activity (Tyr 48, His 110, Lys 77, and Asp 43) are highly conserved. Divergent residues and deletions or insertions are concentrated in the C-terminal region of the protein. This segment of residues which starts at residue 295, forms a loop over the binding pocket which undergoes a shift upon zopolrestat binding in the ALR2 holoenzyme. A similar shift could also occur in FR-1. Aside from the significant variation in sequence at these positions, there are also deletions and insertions in this region which could serve to further modulate substrate specificity and inhibitor binding.

Conclusion. We have demonstrated by crystallographic analysis and activity and inhibition measurements that FR-1 is indeed a catalytic member of the aldo−keto reductase family. Its physiological substrate is unknown, but FR-1 is regulated by a growth factor which is responsible for controlling cell proliferation. The potent inhibitor zopolrestat has been unambiguously shown to bind in the active site of FR-1. Whether this and other aldose reductase inhibitors inhibit the function of diverse members of the aldo−keto reductase enzyme family in human tissues remains to be determined. However, the results of such studies can be expected to have a significant impact on future efforts to enhance the specificity of drugs targeted to aldose reductase for prevention of diabetic complications. High-resolution X-ray structures are required for these efforts.

ACKNOWLEDGMENT

Dr. Jeffrey Winkles is gratefully acknowledged for providing the FR-1 cDNA clone. We thank Terry Griest, Bill Meador, and Tim Reynolds for helpful assistance. Zopolrestat was kindly provided by Pfizer, Inc.

REFERENCES

Anderson, S., Marks, C. M., Lazarus, R., Miller, J., Stafford, K., Seymour, J., Light, D., Rastetter, W., & Estell, D. (1985) *Science 230*, 144−149.

Bachur, N. R. (1976) *Science 193*, 595−597.

Bohren, K. M., Bullock, B., Wermuth, B., & Gabbay, K. H. (1989) *J. Biol. Chem. 264*, 9547−9551.

Bohren, K. M., Grimshaw, C. E., Lai, C.-J., Harrison, D. H., Ringe, D., Petsko, G. A., & Gabbay, K. H. (1994) *Biochemistry 33*, 2021−2032.

Borhani, D. W., Harter, T. M., & Petrash, J. M. (1992) *J. Biol. Chem. 267*, 24841−24847.

Brändén, C. I. (1991) *Curr. Opin. Struct. Biol. 1*, 978−983.

Brünger, A. T. (1992) *X-PLOR: A System for Crystallography and NMR*, Version 3.1 Manual, Yale University Press, New Haven, CT.

Donohue, P. J., Alberts, G. F., Hampton, B. S., & Winkles, J. A. (1994) *J. Biol. Chem. 269*, 8604−8609.

El-Kabbani, O., Green, N. C., Lin, G., Carson, M., Narayanam S. V. L., Moore, K., Flynn, T. G., & DeLucas, L. J. (1994) *Acta Crystallogr. D 50*, 859−868.

Ferrin, T. E., Huang, C. C., Jarvis, L. E., & Langdrige, R. (1988) *J. Mol. Graphics 6*, 13−27.

Fujii, Y., Watanabe, K., Hayashi, H., Urade, Y., Kuramitsu, S., Kagamiyama, H., & Hayashi, O (1990) *J. Biol. Chem. 265*, 9914−9923.

Grimshaw, C. E., Shahbaz, M., & Putney, C. G. (1990) *Biochemistry 29*, 9947−9955.

Gui, T., Tanimoto, T., Kokai, Y., & Nishimura, C. (1995) *Eur. J. Biochem. 227*, 448−453.

Hoog, S. S., Pawlowski, J. E., Alzari, P. M., Penning, T. M. & Lewis, M. (1994) *Proc. Natl. Acad. Sci. U.S.A. 91*, 2517−2521.

Kador, P. F., & Sharpless, N. E. (1983) *Mol. Pharmacol. 24*, 521−531.

Kanazu, T., Shinoda, M., Nakayama, T., Deyashiki, Y., Hara, A., & Sawada, H. (1991) *Biochem J. 279*, 903−906.

Kinoshita, J. H., & Nishimura, C. (1988) *Diabetes/Metab. Rev. 4*, 323−337.

Kubiseski, T. J., Green, N. C., Borhani, D. W., & Flynn, T. G. (1994) *J. Biol. Chem. 269*, 2183−2188.

Merck, K. B., De Haard Hoekman, W. A., & Oude Essink, B. B. (1992) *Biochim. Biophys. Acta 1130*, 267−276.

Morjana, N. A., Lyons, C., & Flynn, T. G. (1989) *J. Biol. Chem. 264*, 2912−2919.

Mylari, B. L., Larson, E. R., Beyer, T. A., Zembrowski, W. J., Aldinger, C. E., Dee, M. F., Siegel, T. W., & Singleton, D. H. (1991) *J. Med. Chem. 34*, 108−122.

Nicholls, A., Sharp, K. A., & Honig, B. (1991) *Proteins 11*, 281−296.

Pailhoux, E. A., Martinez, A., Veyssiere, G. M., & Jean, C. G. (1990) *J. Biol. Chem. 265*, 19932−19936.

Pawlowski, J. E., & Penning, T. M. (1994) *J. Biol. Chem. 269*, 13502−13510.

Pawlowski, J. E., Huizinga, M., & Penning, T. M. (1991) *J. Biol. Chem. 266*, 8820−8825.

Petrash, J. M., Harter, T. M., Devine, C. S., Olins, P. O., Bhatnagar, A., Liu, S. Q., & Srivastava, S. K. (1992) *J. Biol. Chem. 267*, 24833−24840.

Sack, J. S. (1988) *J. Mol. Graphics 6*, 224−245.

Sarges, R. (1989) *Adv. Drug Res. 18*, 139−175.

Sarges, R., & Oates, P. J. (1993) *Prog. Drug Res. 40*, 99−161.

Tarle, I., Borhani, D. W., Wilson, D. K., Quiocho, F. A., & Petrash, J. M. (1993) *J. Biol. Chem. 268*, 25687−25693.

Vander Jagt, D. L., Robinson, B., Taylor, K. K., & Hunsaker, L. A. (1992) *J. Biol. Chem. 267*, 4364−4369.

Watanabe, K., Fujii, Y., Nakayama, K., Ohkubo, H., Kuramitsu, S., Kagamiyama, H., Nakanishi, S., & Hayaishi, O. (1988) *Proc. Natl. Acad. Sci. U.S.A. 85*, 11−15.

Wermuth, B., & Monder, C. (1983) *Eur. J. Biochem. 131*, 423−426.

Wilson, D. K., Bohren, K. M., Gabbay, K. H., & Quiocho, F. A. (1992) *Science 257*, 81−84.

Wilson, D. K., Tarle, I., Petrash, J. M., & Quiocho, F. A. (1993) *Proc. Natl. Acad. Sci. U.S.A. 90*, 9847−9851.

Winters, C. J., Molowa, D. T., & Guzelian, P. S. (1990) *Biochemistry 29*, 1080−1087.

BI951778D